five and seven cycles of freezing and thawing, respectively.

Tests Procedure. The triaxial apparatus was employed as loading system, coupled with a strain-controlled loading mode and an automatic data-collection system. The unconsolidated-undrained triaxial compression (UUTC) experiments were conducted. The confining pressure of triaxial compression is 50 kPa, 150 kPa and 250 kPa, respectively, with the rate of axial strain of 0.8mm/min. The tests were terminated when the axial strain reaches at 15% or appears peak and the axial strain is greater than 5%. The test condition of each specimen is shown in Table 2 in detail.

Table 2. Summary of test condition.

Specimen number	Freeze-thaw cycle	Initial compaction degree (%)	Initial water content (%)	Confine pressure (kPa)
T-01	0	95	12.6	50, 150, 250
T-02	1	95	12.6	50, 150, 250
T-03	3	95	12.6	50, 150, 250
T-04	5	95	12.6	50, 150, 250
T-05	7	95	12.6	50, 150, 250
T-06	3	85	12.6	50, 150, 250
T-07	3	90	12.6	50, 150, 250
T-08	3	100	12.6	50, 150, 250
T-09	3	95	10.0	50, 150, 250
T-10	3	95	14.0	50, 150, 250
T-11	3	95	16.0	50, 150, 250
T-12	3	95	18.0	50, 150, 250

STRESS-STRAIN CURVES OF HARBIN SILTY CLAY

Figure 3 shows the effects of freeze-thaw cycles on stress-strain curves of Harbin silty clay, with compaction degree of 95%, initial water content of 12.6%, and the confining pressure of 50kPa. From this figure, the stress-strain curves of silty clay experienced three to seven freeze-thaw cycles exhibit slight strain-softening. However, the stress-strain curves of silty clay subjected to zero and one freeze-thaw cycle exhibit notably strain-softening in which the peak deviator stress can be observed. Moreover, it is very obvious that the stress-strain curves become stable and the deviator stress display a little change after three freeze-thaw cycles. From these experimental results, they show that the mechanical properties of silty clay soil will be stable after three freeze-thaw cycles. The reason is that the micro-structures of soil are changed by the frost and thaw action. During the freeze process, the free water migrated and frost, and the pore of soil may increase. During the thaw process, the ice crystal melt, and the soil particles rearrange. After many freeze-thaw cycles, the structures of soil become stable, and the mechanical behaviors would not change. The similar results can be found many previous studies (Wang et al, 2007; Su et al., 2008; Yu et al., 2010).

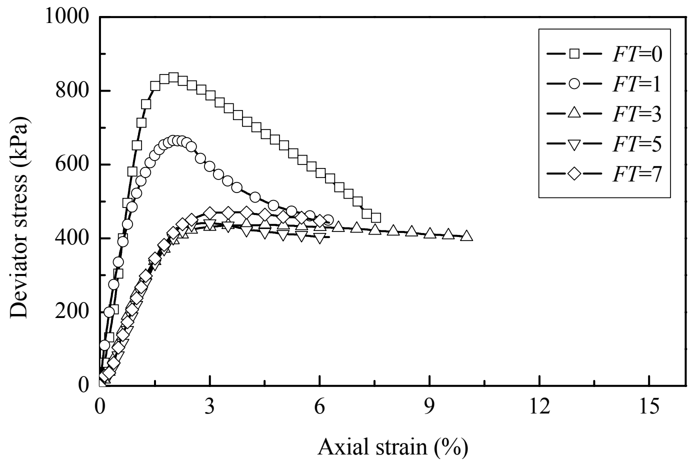

Figure 3. Effects of freeze-thaw cycle on stress-strain curves of Harbin silty clay.

Figure 4 shows the effects of initial compaction degree on stress-strain curves of Harbin silty clay, with three freeze-thaw cycles, initial water content of 12.6% and the confine pressure of 50 kPa. From this figure, it is observed that the stress-strain curves display strain hardening at compaction degree of 85%, but display strain softening at compaction degree of 100%. Moreover, the deviator stress increases with the increasing of initial compaction degree.

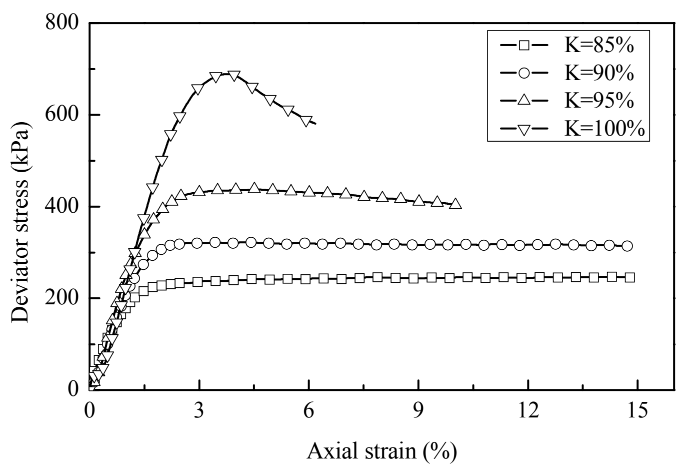

Figure 4. Effects of initial compaction degree on stress-strain curves of Harbin silty clay.

Figure 5 shows the effects of initial water content on the stress-strain curves of Harbin silty clay, with three freeze-thaw cycles, the compaction degree of 95% and the confining pressure of 50 kPa. After three freeze-thaw cycles, the initial water content plays a notable effect on the stress-strain curves mode. Whether strain is hardening or softening mode, it depends on the initial water content. Additionally, the peak deviator stress increases with the decreasing of the water content.

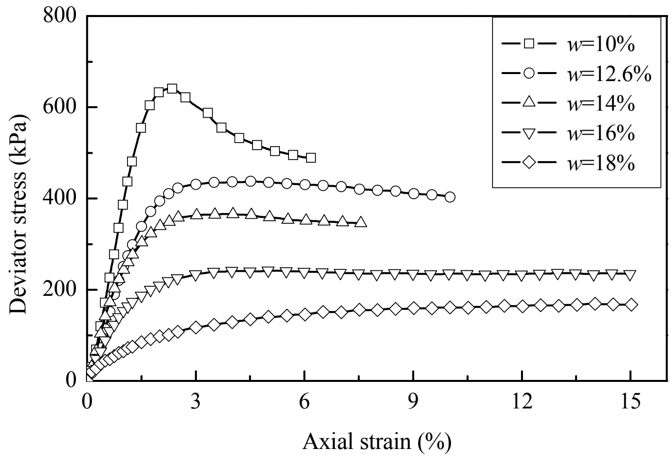

Figure 5. Effects of initial water content on stress-strain curves of Harbin silty clay.

FAILURE STRENGTH AND TANGENT MODULUS

Failure strength and modulus are two important parameters of soil mechanical properties. The resilient modulus of cohesive soil can be estimated by the stress level at 1% strain in UC test (Lee et al., 1995), and Wang et al. (2007) defined the resilient modulus as a ratio of deviator stress increment at 1% axial strain to axial strain increment relate to initial value. In the present study, the modulus of Harbin silty clay is defined as the tangent modulus of the deviator stress at 1% axial strain. Failure strength is the deviator stress at the axial strain of 15% for the strain-hardening mode curve, and is the peak deviator stress for the strain-softening mode curve.

Figure 6 shows failure strength and tangent modulus for various numbers of freeze-thaw cycles. The failure strength decreased with the increasing of number of freeze-thaw cycle, and it is stable basically after three freeze-thaw cycles. The strengthen decrease by 48%, 36% and 35% after three freeze-thaw cycles at confining pressure of 50 kPa, 150 kPa and 250 kPa, respectively. Moreover, It is obvious that the tangent modulus notably affected by freeze-thaw action. The tangent modulus of soil decreases by 50~62% at various after three freeze-thaw cycles, and then change a little at rest freeze-thaw cycles action.

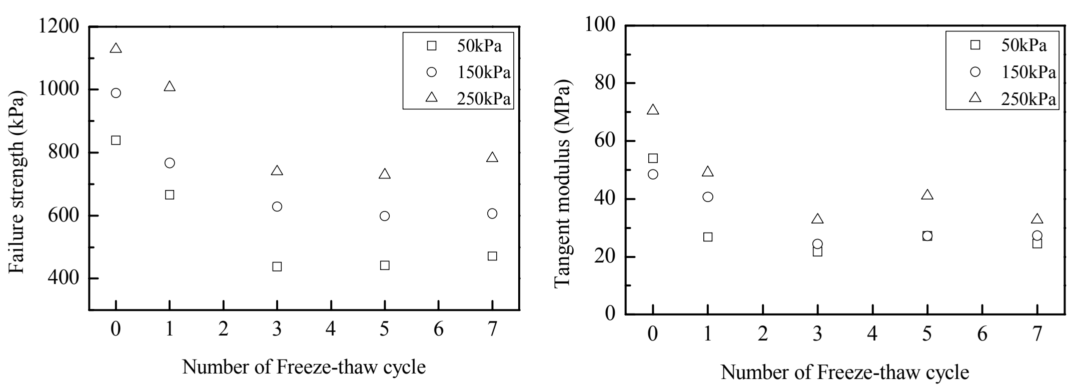

Figure 6. Effects of freeze-thaw cycles on failure strength and tangent modulus.

Figure 7 shows failure strength and tangent modulus of Harbin silty clay, with three freeze-thaw cycles and initial water content of 12.6%, for various initial compaction degree. The failure strength and tangent modulus of soil increases with increasing of initial compaction degree and confining pressure.

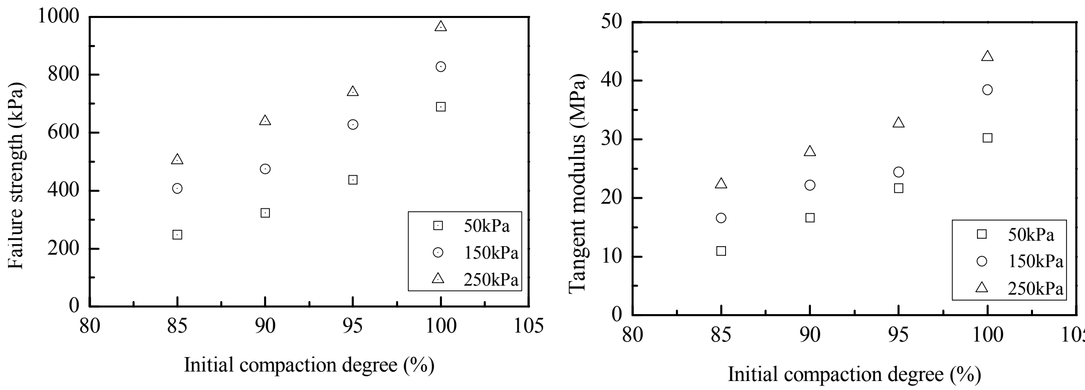

Figure 7. Effects of initial compaction degree on failure strength and tangent modulus.

Figure 8 shows failure strength and tangent modulus, with three freeze-thaw cycles and compaction degree of 95%, for various initial water content. It is clear from this figure that failure strength and tangent modulus decrease with increasing of water content.

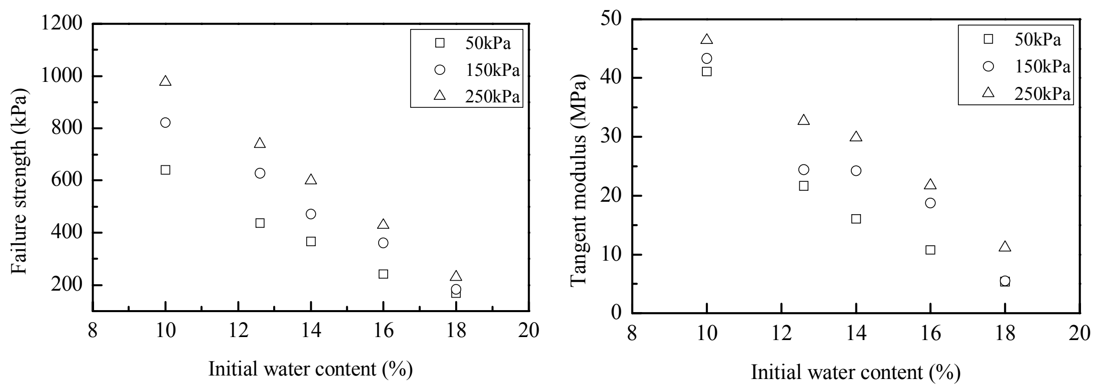

Figure 8. Effects of initial water content on failure strength and tangent modulus.

EMPIRICAL MODEL AND VALIDATION

Normalized Failure Strength and Normalized Tangent Modulus. To determine the standard failure strength q_{Nf} and standard tangent modulus E_{Nt}, Equation (1) and Equation (2) were applied and fitted to all of the failure strength and the tangent modulus under different experiments conditions, respectively. Then the relationships between the failure strength and confining pressure, the tangent modulus and confining pressure were proposed, respectively.

$$q_{Nf} = K_f \cdot p_a \cdot \left(\frac{\sigma_3}{p_a}\right)^m \tag{1}$$

$$E_{Nt} = K_t \cdot p_a \cdot \left(\frac{\sigma_3}{p_a}\right)^n \tag{2}$$

Where q_{Nf} is standard failure strength, E_{Nt} is standard tangent modulus, σ_3 is confining pressure, p_a is standard pressure generally with 100 kPa, K_f, K_t, m and n are material constants with K_f=5.50, K_t=272.95, m=0.29 and n=0.25, respectively. These material constants were determined by fitting the relationship of failure strength, tangent modulus and confining pressure.

Figure 9 shows normalized failure strength and normalized tangent modulus of soil for various numbers of freeze-thaw cycles. It is obvious that the normalized failure strength and normalized tangent modulus decreases with the increasing of numbers of freeze-thaw cycles, and the curve is stable after three freeze-thaw cycles. The relationship of normalized failure strength, normalized tangent modulus and numbers of freeze-thaw cycle can be fitted by Equation (3) and Equation (4) as follows, respectively.

$$g_N = \frac{q_f}{q_{Nf}} = A_1 \cdot e^{A_2 \cdot N} + 1 \tag{3}$$

$$f_N = \frac{E_t}{E_{Nt}} = e^{C_1 \cdot N} + C_2 \tag{4}$$

Where g_N is normalized failure strength effected by number of freeze-thaw cycle, f_N is normalized tangent modulus effected by number of freeze-thaw cycle, q_f is failure strength, E_t is tangent modulus, N is numbers of freeze-thaw cycle, A_1, A_2, C_1 and C_2 are model parameters with A_1=0.69, A_2=-0.75, C_1=-1.23 and C_2=0.99, respectively.

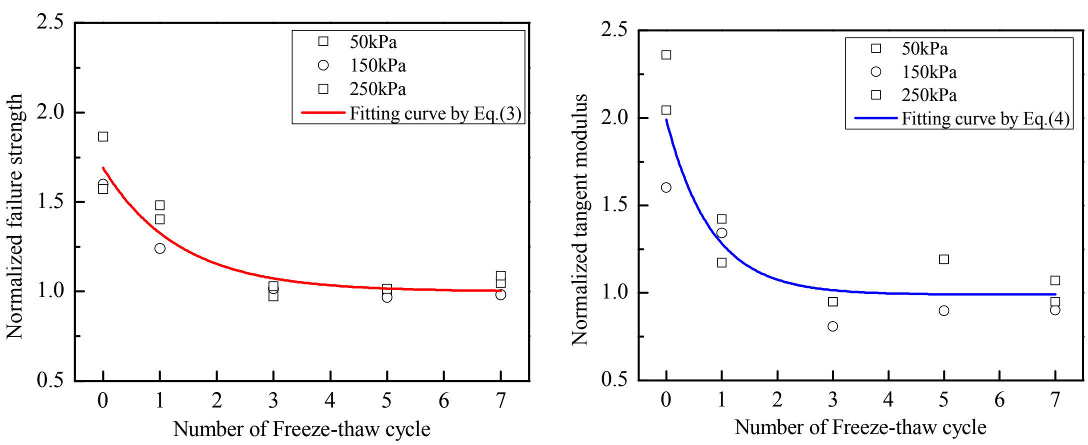

Figure 9. Effects of freeze-thaw cycles on normalized failure strength and normalized tangent modulus.

Figure 10 shows normalized failure strength and normalized tangent modulus of soil for various initial compaction degree. It obvious the normalized failure strength and normalized tangent modulus increases with the increasing of initial compaction degree. The relationship of normalized failure strength, normalized tangent modulus and initial compaction degree can be fitted by Equation (5) and Equation (6) as follows.

$$g_K = \frac{q_f}{q_{Nf}} = A_3 \cdot e^{A_4 \cdot K} \tag{5}$$

$$f_K = \frac{E_t}{E_{Nt}} = C_3 \cdot e^{C_4 \cdot K} \tag{6}$$

Where g_K is normalized failure strength effected by initial compaction degree, f_K is normalized tangent modulus effected by initial compaction degree, K is initial compaction degree of soil, A_3, A_4, C_3 and C_4 are model parameters with A_3=0.0071, A_4=5.26, C_3=0.0055 and C_4=5.42.

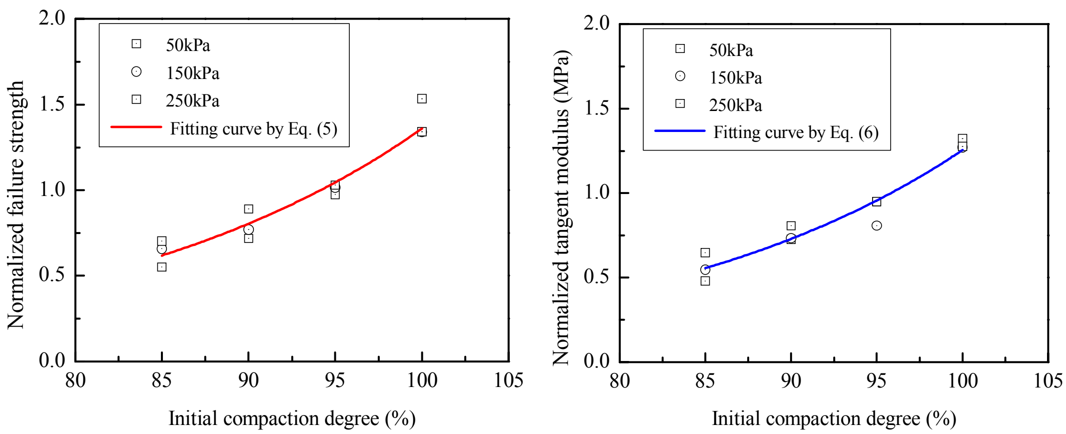

Figure 10. Effects of initial compacted degree on normalized failure strength and normalized tangent modulus.

Figure 11 shows normalized failure strength and normalized tangent modulus of soil for initial water content. It obvious the normalized failure strength and normalized tangent modulus decreases with the increasing of initial water content. The relationship of normalized failure strength and initial water content displays linear dependence, and the relationship of normalized tangent modulus and initial water content displays exponential dependence.

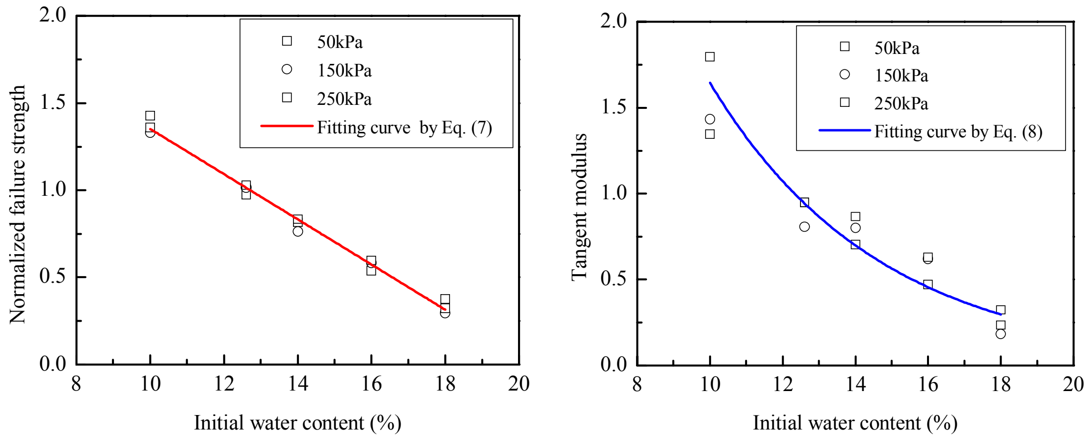

Figure 11. Effects of initial water content on normalized failure strength and normalized tangent modulus.

The relationship of normalized failure strength, normalized tangent modulus and initial compaction degree can be fitted by Equation (7) and Equation (8) as follows.

$$g_w = \frac{q_f}{q_{Nf}} = A_5 \cdot w + A_6 \quad (7)$$

$$f_w = \frac{E_t}{E_{Nt}} = C_5 \cdot e^{C_6 \cdot w} \quad (8)$$

Where g_w is normalized failure strength effected by initial water content, f_w is normalized tangent modulus effected by initial water content, w is initial water content, A_5, A_6, C_5 and C_6 are model parameters with A_5=-12.98, A_6=2.65, C_5=14.02 and C_6=-21.42, respectively.

Model and Validation. Basic structure of failure strength and tangent modulus of Harbin silty clay subjected to freeze-thaw cycle is composed of one modification parameter and three modification functions. The parameters and functions of normalized failure strength and normalized tangent modulus were discussed in above and are shown from Equation (1) to Equation (8). The failure strength and tangent modulus model are written as follows in Equation (9) and Equation (10).

$$q_f = \lambda \cdot q_N \cdot q_K \cdot q_w \cdot q_{Nf} = \lambda \cdot K_f \cdot p_a \cdot g_N \cdot g_K \cdot g_w \cdot \left(\frac{\sigma_3}{p_a}\right)^m \quad (9)$$

$$E_t = \eta \cdot f_N \cdot f_K \cdot f_w \cdot E_{Nt} = \eta \cdot K_t \cdot p_a \cdot f_N \cdot f_K \cdot f_w \cdot \left(\frac{\sigma_3}{p_a}\right)^n \quad (10)$$

Where λ is modification parameter with 0.92 for failure strength, η is modification parameter with 1.08 for tangent modulus, q_{Nf} is normalized parameter which is determined by Equation (1), E_{Nt} is normalized parameter which is determined by Equation (2), g_N, g_K, g_w, f_N, f_K and f_w are modification functions influenced by numbers of freeze-thaw cycle, initial compaction degree and initial water content, respectively.

For the validation of the models which are proposed in this paper, the comparison of the experimental results and the calculated results through the Equation (9) and Equation (10) are shown in Figure 12. From the figure, the overall agreement between the model and experimental data can be called well, although some calculated data depart experimental data. This demonstrates that the presented failure strength and tangent modulus model are suitable for the description of failure strength and tangent modulus of compacted soil for various numbers of freeze-thaw cycle, initial compaction degree and initial water content.

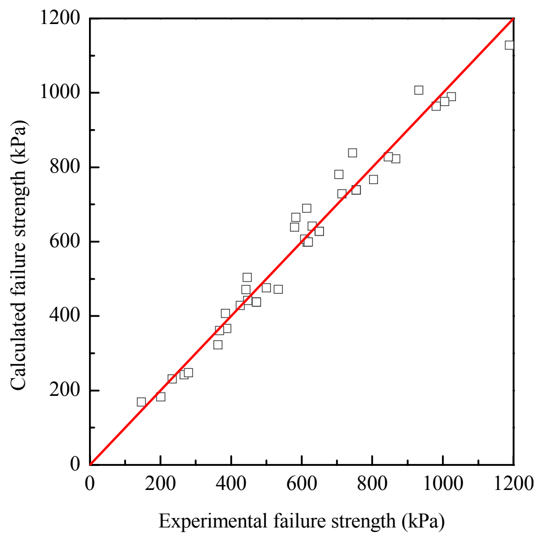

Figure 12. Comparison of experimental results and calculated results.

CONCLUSIONS

An unconsolidated-undrained triaxial compression experiments were conducted on compacted Harbin silty clay, the effect of the stress-strain curve, failure strength and tangent modulus on different confining pressure, number of freeze-thaw cycle, initial compaction degree and initial water content were investigated. The following conclusions are drawn based on this study:

(1) The confining pressure, number of freeze-thaw cycle, initial compaction degree and initial water content are notable effect the stress-strain curve mode, such as strain-hardening and strain-softening.

(2) Failure strength and tangent modulus are stable after three freeze-thaw cycles, and decrease by 35~48% and 50~62% of the strength of un-experienced freeze-thaw cycle, respectively. Failure strength and tangent modulus increase notably with the increasing of initial compaction degree and decrease notably with the increasing of initial water content. Moreover, the normalized failure strength and tangent modulus display similar rules.

(3) The empirical models of failure strength and tangent modulus were proposed and validated based on experimental results. They can consider the effects of the confining pressure, number of freeze-thaw cycle, initial compaction degree and initial water content.

ACKNOWLEDGEMENTS

This research is supported by the National Key Basic Research Development Plan (2012CB026104), the National Science and Technology Support Project (No. 2014BAG05B07), the National Natural Science Foundation of China (No. 41430634, 51408163), the Natural Science Foundation of Heilongjiang Province (No. ZD201218), China Postdoctoral Science Foundation Funded Project (No. 2012M520751), and the Fundamental Research Funds for the Central University (No. HIT. NSRIF. 2014078).

REFERENCES

Cui, Z. D., He, P. P., and Yang, W. H. (2014). "Mechanical properties of a silty clay subjected to freezing-thawing." *Cold Regions Science and Technology*, Vol. 98: 26-34.

Ishikawa, T., Ozaki, Y., and Miura, S. (2008). "Influence of freeze-thaw action on mechanical behavior of crushable volcanic coarse-grained soils." *Journal of Geotechnical and Geoenvironmental Engineering, JSCE*, Vol. 64(3): 712-717.

Lee, W., Bohra, N. C., Altschaeff, A. G., and White, T. D. (1995). "Resilient modulus of cohesive soils and the effect of freeze-thaw." *Canadian Geotechnical Journal*, Vol. 32, 559-568.

Li, G. Y., Ma, W., Zhao, S. P., Mao, Y. C. and Mu Y. H. (2012). "Effect of freeze-thaw cycle on mechanical behavior of compacted fine-grained soil." *Cold Regions Engineering 2012: Sustainable Infrastructure Development in a Changing Cold Environment*, 72-81.

Liu, J. K., and Peng, L. Y. (2009). "Experimental study on the unconfined compression of a thawing soil." *Cold Regions Science and Technology*, Vol. 58: 92-96.

Qi, J. L., Ma, W., and Song, C. X. (2008). "Influence of freeze-thaw on engineering properties of a silty soil." *Cold Regions Science and Technology*, Vol. 53: 397-404.

Qi, J. L., Zhang, J. M., and Zhu, Y. L. (2004). "Influence of freezing-thawing on soil structure and its soils mechanics significance." *Chinese Journal of Rock Mechanics and Engineering*, Vol. 23(s2), 2690-2694.

Simonsen, E., Janoo, V. C., and Isacsson, U. (2002). "Resilient properties of unbound road materials during seasonal frost conditions". *Journal of Cold Regions Engineering,* Vol. 16(1): 28-50.

Su, Q., Tang, D. and Liu, S. (2008). "Test on physic-mechanical properties of Qinghai-Tibet slope clay under freezing-thawing cycles." *Chinese Journal of Rock Mechanics and Engineering*, Vol. 27(s1): 2990-2994.

Viklander, P. (1998). "Permeability and volume changes in till due to cyclic freeze-thaw." *Canadian Geotechnical Journal.* Vol. 35 (3):471-477.

Wang, D.Y., Ma, W., Niu, Y. H. Chang, X. X., and Wen, Z. (2007). "Effects of cyclic freezing and thawing on mechanical properties of Qinghai-Tibet clay." *Cold Regions Science and Technology*, Vol. 48(1): 34-43.

Yu, L. L., Xu, X. Y., Qiu, M. G., Yan, Z. L., and Li, P. F. (2010). "Influence of freeze-thaw on shear strength properties of saturated silty clay." *Rock and Soil Mechanics*, Vol. 31(8): 2448-2452.